AJNR

Decline in Corpus Callosum Volume among Pediatric Patients with Medulloblastoma: Longitudinal MR Imaging Study

Shawna L. Palmer, Wilburn E. Reddick, John O. Glass, Amar Gajjar, Olga Goloubeva and Raymond K. Mulhern

AJNR Am J Neuroradiol 2002, 23 (7) 1088-1094
http://www.ajnr.org/content/23/7/1088

AJNR Am J Neuroradiol 23:1088–1094, August 2002

Decline in Corpus Callosum Volume among Pediatric Patients with Medulloblastoma: Longitudinal MR Imaging Study

Shawna L. Palmer, Wilburn E. Reddick, John O. Glass, Amar Gajjar, Olga Goloubeva, and Raymond K. Mulhern

BACKGROUND AND PURPOSE: **A decline in intrahemispheric cerebral white matter volume in children treated for brain tumors with cranial irradiation has been well documented. It was hypothesized that the development of the corpus callosum, the largest white matter commissure of the brain, would also be adversely affected after treatment with cranial irradiation in pediatric patients treated for medulloblastoma.**

METHODS: **After diagnosis, 35 patients (22 male and 13 female patients) with histologically proved medulloblastoma were treated by maximal surgical resection, risk-adapted craniospinal irradiation, and chemotherapy. Using quantitative measurement techniques with MR imaging, corpus callosum volume was measured at multiple time points for each patient during a 4-year period.**

RESULTS: **Quantitative MR imaging analyses of 239 examinations in 35 patients showed, in contrast to normal development, that the total midsagittal corpus callosum area decreased with time from craniospinal irradiation (–18.0 mm^2/y; $P < .0001$). After examination of seven corpus callosum subregions, significant declines were also observed: genu (–2.2 mm^2/y; $P = .03$), rostral body (–2.0 mm^2/y; $P = .04$), anterior midbody (–1.4 mm^2/y; $P = .005$), posterior midbody (–1.2 mm^2/y; $P = .004$), isthmus (–2.4 mm^2/y; $P = .001$), and splenium (–5.0 mm^2/y; $P = .007$).**

CONCLUSION: **The greatest deviation from normal development occurred in the most posterior subregions of the corpus callosum: the isthmus and the splenium. These corpus callosum subregions, associated with fibers traversing from the temporal, posterior parietal, and occipital lobes, are normally expected to have the highest rate of growth during childhood. However, these regions also received the highest total dose of irradiation, providing a possible explanation for atypical corpus callosum development observed in these 35 patients treated for medulloblastoma.**

Standard therapy for medulloblastoma includes maximal surgical resection of the tumor and postoperative craniospinal irradiation (CSI), including a boost to the posterior fossa, with adjuvant chemotherapy. It has been well documented in the literature that CSI is associated with several CNS abnormalities, such as cerebral atrophy, focal and diffuse white matter lesions, and enlarged ventricles (1). Patients treated with surgery and CSI exhibit reduced white matter volume compared with that of patients treated with surgery alone (2). In addition, loss of intrahemispheric white matter volume has been shown to be dose dependent, with those receiving conventional CSI doses (36 Gy) exhibiting steeper declines than those receiving reduced CSI doses (23.4 Gy) (3). It is generally accepted that damage to the microvasculature and accompanying injury to glial cells are among the underlying mechanisms involved in such damage (4). As the primary white matter commissure of the brain, consisting of approximately 180 million myelinated axons (5), the corpus callosum is vulnerable to CSI-related damage. The corpus callosum mediates a large number of cortical processing areas in each hemisphere. Damage could therefore interrupt these

Received October 2, 2001; accepted after revision March 14, 2002.

From the Division of Behavioral Medicine (S.L.P., R.K.M.) and the Departments of Diagnostic Imaging (W.E.R., J.O.G.), Hematology/Oncology (A.G.), and Biostatistics and Epidemiology (O.G.), St. Jude Children's Research Hospital; the Department of Pediatrics (A.G., R.K.M.), University of Tennessee College of Medicine; and the Departments of Electrical and Computer Engineering and Biomedical Engineering (W.E.R.), University of Memphis, Memphis, TN.

Supported by the National Cancer Institute through a Cancer Center Support (CORE) grant (P30-CA21765) and by the American Lebanese Syrian Associated Charities.

Address reprint requests to Shawna L. Palmer, PhD, Division of Behavioral Medicine, St. Jude Children's Research Hospital, 332 N. Lauderdale, Memphis, TN 38105-2794.

important pathways, leading to difficulties in neurocognitive performance.

Using quantitative measurement techniques with MR imaging (6, 7), the present study focused on measures of the corpus callosum obtained at multiple time points for each patient. The primary objective was to examine the growth patterns of the corpus callosum during a 4-year period since the start of treatment with CSI among pediatric patients with medulloblastoma and to compare these patterns with known normal growth patterns (8). Considering the CSI dose distribution used in the treatment of medulloblastoma, it was hypothesized that the posterior regions of the corpus callosum would show the greatest deviations from normal development. A secondary objective was to examine the impact of two known risk factors in this population: young age at the time of CSI treatment and higher CSI dose (3, 9, 10). It was hypothesized that those who were younger at the start of the CSI treatment and those who received higher (conventional) dose CSI would show greater deviations from normal development than those receiving reduced dose CSI.

Methods

Patient Characteristics

Patients were drawn from an internal review board–approved institutional protocol for newly diagnosed medulloblastoma arising in the posterior fossa. Patients in whom medulloblastoma was diagnosed after three and before 21 years of age and who were 1 or more years from the start of therapy were considered eligible for the study (n = 36). After presentation, all patients were treated by maximal surgical resection of the tumor. All patients then received risk-adapted CSI (11). Patients at average risk (those with total tumor resection and no dissemination) received 23.4-Gy CSI, and patients at high risk (those with either subtotal tumor resection or metastatic disease) received an up-front phase II window of topotecan and then 36- to 39.6-Gy CSI. All patients also received a posterior fossa boost to 55.8 Gy. Six weeks after completion of the radiation treatment, patients at average risk and patients at high risk started adjuvant chemotherapy that comprised four cycles of high-dose cyclophosphamide, cisplatin, and vincristine. After each chemotherapy cycle, infusion of peripheral blood stem cells or autologous bone marrow was performed (12).

Each patient underwent protocol-driven serial MR imaging examinations. These examinations were scheduled to occur every 3 months for the first 2 years and every 6 months for the next 5 years. Multiple images were collected for all 36 of the eligible patients. However, for the purpose of this analysis, each patient had to undergo at least three MR imaging examinations for inclusion in the study. One patient had excessive motion during four of his five MR imaging examinations, which prevented accurate processing; that patient was therefore excluded from the study. Examinations showing evidence of progressive disease, and any subsequent examinations, were not included in the analysis. MR studies included 239 examinations of 35 patients (range, three to 13 examinations per patient; median, seven examinations per patient).

MR Imaging

Imaging was performed on a 1.5-T Magnetom (Siemens Medical Systems, Iselin, NJ) whole-body unit with the standard circular polarized volume head coil. T1-weighted images were acquired in the sagittal plane as 5-mm-thick sections with a 1-mm gap. A single sagittal image was selected as the midline section for analysis. Criteria for choosing the midline section were the patency of the cerebral aqueduct and the presence of the septum pellucidum.

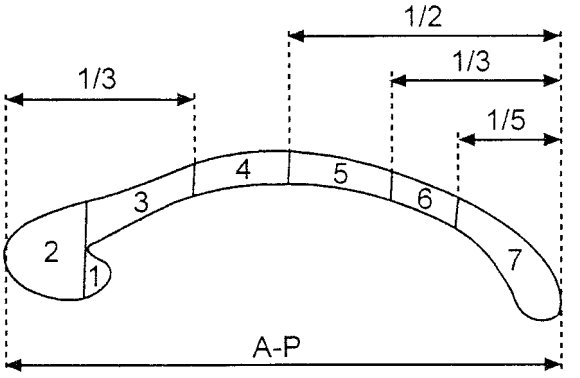

FIG 1. Corpus callosum subregions. *1*, rostrum; *2*, genu; *3*, rostral body; *4*, anterior midbody; *5*, posterior midbody; *6*, isthmus; and *7*, splenium. Based on division of the longest anteroposterior (*A-P*) line.

Quantitative MR Image Processing

Using a fully automated segmentation algorithm (7) and manual classification, the area of the corpus callosum was derived from the midline sagittal section. The corpus callosum and immediate surrounding tissue was first manually designated as the region of interest. Segmentation of the region of interest, the process by which the area is decomposed into similar regions on the basis of signal intensity by an automated algorithm, was then completed. The segmentation procedure, linear vector quantitization, used T1 signal intensities as input to produce nine output vectors. Each of the nine output vectors from the segmented image was then classified as either corpus callosum tissue, partial volume of corpus callosum and gray matter, partial volume of corpus callosum and CSF, or background. The vectors associated with the partial volume region were set to zero to produce an equivalent null vector. The segmentation algorithm was executed again, forcing each pixel in the null vector to be assigned to the nearest output, classified as either corpus callosum or background. This resulted in two regions: corpus callosum, which was colored green, or background, which was colored black. A histogram for the color green was then completed to determine the number of pixels present. The pixel count was multiplied by pixel area, resulting in corpus callosum area for the midline section.

Using linear distances to divide the corpus callosum (13), areas of seven corpus callosum subregions were also calculated (Fig 1). After segmentation and classification of the corpus callosum, divisions were automatically placed on the image by a C-language software program specifically designed to run on a UNIX system. This software first found the longest anteroposterior line in the corpus callosum image. The slope of this line was then calculated, and perpendicular lines to delineate the seven subregions were then placed along the anteroposterior line. After transfer of the image to a personal computer, the seven subregions were then individually selected with the standard tools of Photoshop, and pixel counts were obtained. With image dimension and field-of-view information, these pixel counts were then converted to area measures. Total postprocessing time for each MR image was approximately 12 to 15 minutes.

All segmentation and classification in this study was completed by one observer (S.L.P.). To test accuracy, total volume measures derived from traditional hand-tracing techniques by an expert observer (W.E.R.) were completed on 10 randomly selected cases, each traced five times. These measures were

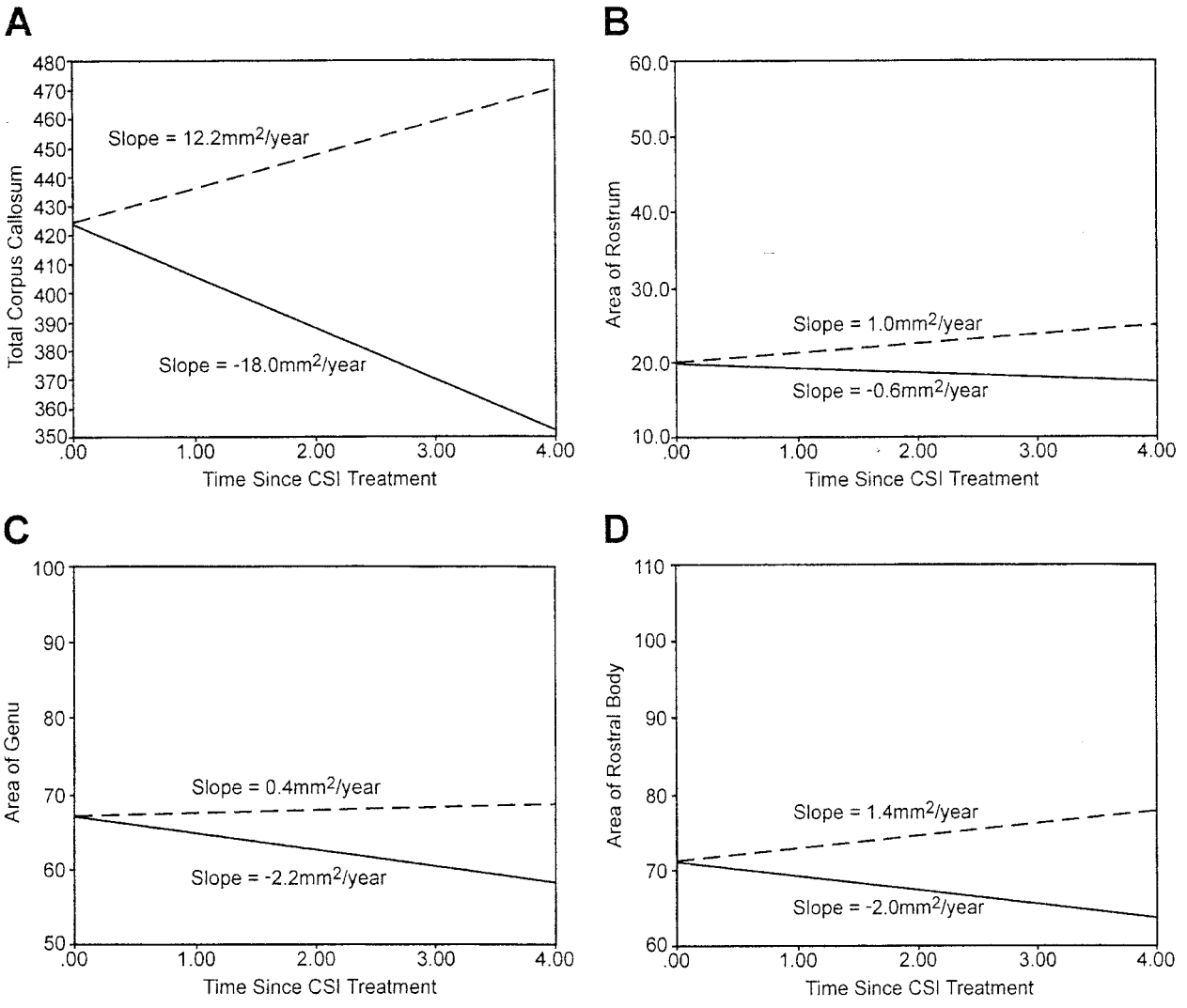

FIG 2. Expected growth (mm^2/y) for the normal population (*dashed line*) and obtained growth among the patients with medulloblastoma (*solid line*) over time (in years) from the start of craniospinal irradiation. *A*, total corpus callosum; *B*, rostrum; *C*, genu; and *D*, rostral body.

compared with those derived from the automated segmentation and manual classification process (S.L.P.), resulting in a correlation coefficient of $r = 0.98$ ($P < .001$). Intraobserver reliability (S.L.P.) was established with five randomly selected cases, each processed five times. The intraclass correlation coefficient for consistency was 0.94 ($P < .0001$). Twenty MR imaging examinations were randomly selected from the dataset and independently processed by two trained observers (S.L.P., W.E.R.) by using the automated segmentation and manual classification process to establish interobserver reliability. A correlation of 0.97 was derived by using the Spearman-Brown method of deriving effective reliability (14).

Researchers from the National Institutes of Health have used the same method of corpus callosum division to obtain normal age-related patterns of corpus callosum growth (8). For purposes of comparison, the growth patterns obtained from the normal population were plotted against the growth patterns obtained from the patients with medulloblastoma.

Statistical Analysis

The primary objective was to examine the growth pattern of the corpus callosum area over time since the start of CSI. Growth curve analysis of longitudinal data, as used in this study, is a common application of random-effects models. The regression model from each patient is assumed to be a random deviation from the population regression model. This approach emphasizes the explanation of within-person variation by the natural development process, with each patient serving as his or her own control (15–20).

The primary covariate included in the model was time from CSI. The two plausible risk factors for this population, young age at CSI treatment and higher CSI dose, were also included in the model. For the purpose of analysis, patients were assessed according to median age at the start of CSI (≤6.88 years versus >6.88 years) and CSI dose (23.4 Gy versus 36–39.6 Gy).

All analyses tested the null hypothesis (slope = 0). This was considered a conservative approach compared with normal neurodevelopmental expectations of the corpus callosum, as analysis of historical controls show an increasing pattern of development over time (8).

Results

Patient Characteristics

Of the 35 eligible patients with medulloblastoma, 22 were at average risk and 13 were at high risk. Twenty-two patients were male and 13 female; 24 were Cauca-

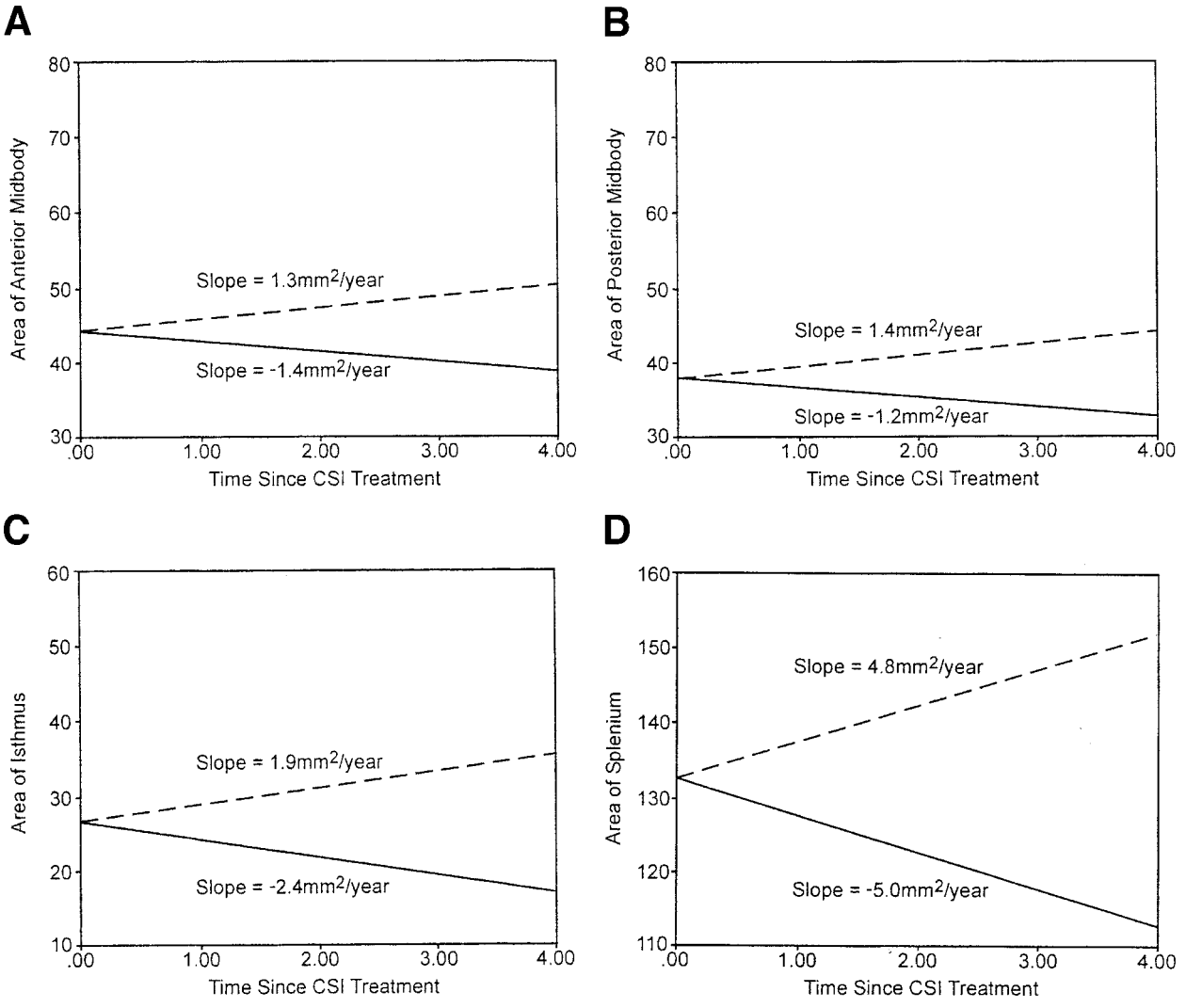

FIG 3. Expected growth (mm^2/y) for the normal population (*dashed line*) and obtained growth among the patients with medulloblastoma (*solid line*) over time (in years) from the start of craniospinal irradiation. *A*, anterior midbody; *B*, posterior midbody; *C*, isthmus; *D*, splenium.

sian, eight African-American, and three Hispanic. The mean age at the start of CSI was 7.68 years (SD = 3.25 years; median, 6.88 years; range, 3.2–17.2 years). At the time of their most recent MR imaging examination, patients were a mean of 9.61 years of age (SD = 3.77 years) and were a mean of 1.92 years from the start of their radiation therapy (SD = 0.97).

Corpus Callosum Measures

The growth patterns for the midsagittal corpus callosum areas obtained from the medulloblastoma patient group were compared with the growth patterns of the midsagittal corpus callosum areas expected in the normal population (8). For each corpus callosum region, the rate of change for the medulloblastoma patient group was negative in contrast to the rate of change in the normal population that showed an increasing pattern over time. Normal developmental expectation for total corpus callosum is a significant gain of 12.2 mm^2/y ($P = .0001$). In contrast, the patient with medulloblastoma experienced a significant loss of 18.0 mm^2/y ($P < .0001$) (Fig 2A). Although the rostrum and genu of the normal population showed insignificant increases over time, in the medulloblastoma patient group, the rostrum showed an insignificant decrease, and the genu showed a significant decrease ($P = .03$) (Fig 2B and C). The normal population exhibited a significant increase for the rostral body ($P = .04$). In contrast, the medulloblastoma patient group showed a significant loss for the rostral body ($P = .04$) (Fig 2D). The pattern of growth for the anterior and posterior midbody among the normal population showed a significant increase ($P = .0001$), whereas the pattern of growth among the medulloblastoma patient group showed a significant decrease ($P = .005$ and $P = .004$, respectively) (Fig 3A and B). For the isthmus, a significant increase is expected within the normal population ($P = .0001$); however, the medulloblastoma group showed a significant decrease ($P = .001$) (Fig 3C). Finally, the

TABLE 1: Differences in slopes between patients who received reduced (23.4 Gy) or conventional (36–39.6 Gy) craniospinal irradiation doses

CC Region	CSI Dose (Gy)	Slope*	Significance†
Total	Reduced	−20.0	0.52
	Conventional	−16.0	
Rostrum	Reduced	0.2	0.29
	Conventional	1.4	
Genu	Reduced	−0.1	0.20
	Conventional	−4.6	
Rostral body	Reduced	−2.4	0.55
	Conventional	−1.2	
Anterior midbody	Reduced	−1.6	0.81
	Conventional	−1.2	
Posterior midbody	Reduced	−1.4	0.98
	Conventional	−1.4	
Isthmus	Reduced	−2.0	0.75
	Conventional	−2.2	
Splenium	Reduced	−7.0	0.17
	Conventional	−2.4	

Note.—CC indicates corpus callosum; CSI, craniospinal irradiation.

* Change in CC size per year since start of CSI (mm^2).

† Testing H_0: slope (reduced) = slope (conventional); $P < .05$, two-tailed test.

TABLE 2: Differences in slopes between patients who were younger (≤6.8 years) or older (>6.8 years) at the start of craniospinal irradiation

CC Region	Age at CSI	Slope*	Significance†
Total	Younger	−24.0	0.27
	Older	−16.0	
Rostrum	Younger	−0.6	0.24
	Older	1.0	
Genu	Younger	−4.4	0.56
	Older	−2.4	
Rostral body	Younger	−1.8	0.92
	Older	−2.0	
Anterior midbody	Younger	−2.2	0.42
	Older	−1.2	
Posterior midbody	Younger	−1.4	0.97
	Older	−1.4	
Isthmus	Younger	−2.8	0.56
	Older	−2.0	
Splenium	Younger	−13.4	0.09
	Older	−4.8	

Note.—CC indicates corpus callosum; CSI, craniospinal irradiation.

* Change in CC size per year since start of CSI (mm^2).

† Testing H_0: slope (reduced) = slope (conventional); $P < .05$, two-tailed test.

splenium showed a significantly increasing pattern in the normal population ($P = .0001$), whereas it showed a significantly decreasing pattern in the medulloblastoma group ($P = .007$) (Fig 3D).

Analysis of Risk Factors

The trajectory of change in the corpus callosum area was modeled over time from the start of CSI. Both risk factors, CSI dose and age at the start of CSI, were included in the model. Patients who received reduced CSI doses of 23.4 Gy (n = 22) were compared with those who received conventional doses of 36 to 39.6 Gy (n = 13). No sufficient evidence was found to conclude that CSI dose had an impact on corpus callosum development. The average volumes declined at similar rates in both groups (Table 1).

Patients with medulloblastoma who were at or below the median age at the start of CSI (≤6.88 years) were compared with those who were above the median age at the start of CSI (>6.88 years). Although the younger patients showed a trend toward greater declines over time than did patients in the older group, no statistically significant effects were found for age at CSI; both groups declined at similar rates for all corpus callosum regions (Table 2).

Discussion

To our knowledge, the present study is the first to evaluate patterns of corpus callosum development among children treated for brain tumors, specifically 35 patients who received CSI during treatment for pediatric medulloblastoma of the posterior fossa region. Using the longitudinal analyses of 239 MR imaging examinations, the total midsagittal area of the corpus callosum was found to significantly decrease across time since the start of CSI. Examination of the corpus callosum subregions revealed that significant declines in the midsagittal area had occurred over time since the start of CSI for the genu, rostral body, anterior midbody, posterior midbody, isthmus, and splenium. These declining patterns were in marked contrast to expected positive corpus callosum growth in the normal population. Normal development of the corpus callosum reflects an anterior to posterior pattern, with the most anterior regions (rostrum, genu) reaching a plateau during the early preschool years (5, 8). Total corpus callosum volume continues to increase throughout the adolescent years, largely facilitated by moderate growth of the anterior and posterior midbody and robust growth of the posterior isthmus and splenium regions (5). These differential patterns of corpus callosum growth are thought to be the direct result of myelination of callosal axons present at birth.

Quantitative MR imaging techniques have been used to examine corpus callosum volumetry in special settings to measure response to both external environmental and internal organic conditions. Although enriched environments were found to relate to increased corpus callosum size in rats (21), prenatal cranial irradiation has been found to cause callosal neuronal death, postnatal axonal elimination, and, in many cases, especially for those receiving high doses, completely restricted corpus callosum development (22). In studies of the human corpus callosum, a reduced corpus callosum area, associated with demyelination, has been shown among patients with adrenoleukodystrophy, the most common leukodystrophy in children (23). MR imaging in this population shows T2 prolongation during early stages of the disease that may indicate demyelination, inflammatory infil-

trate, or both. A reduction in posterior corpus callosum regions (24) and anterior corpus callosum regions (25) has been shown among autistic persons. Similar results have also been found among those with attention deficit hyperactivity disorder (26–28). Reduced total midsagittal area and reduced splenium and isthmus area of the corpus callosum have also been found among patients with Williams syndrome (29).

The posterior regions of the corpus callosum are expected to have the highest rate of potential growth during childhood (5, 8). Because the medulloblastoma tumor bed is in the posterior fossa region, the posterior regions of the corpus callosum are expected to receive highest amounts of irradiation during CSI. Therefore, irradiation exposure may explain the greater deviations from normal development seen in the posterior regions of the corpus callosum. Previous literature has shown differential dose effects on white matter volume and that these white matter changes tend to increase as time from treatment lengthens (3). The present study shows a relatively early deviation from normal corpus callosum development but fails to find a significant difference between CSI dose subgroups. Differences between the two subgroups may be more marked over time. Reevaluation of the data as more time elapses from initiation of treatment is warranted.

Decline in corpus callosum volume stemming from treatment for medulloblastoma may have neuropsychological implications. In a late effects study of 19 adolescents who had experienced traumatic brain injury, it was found that corpus callosum area measures were strongly correlated with measures of intellectual functioning, verbal learning and memory, visuospatial ability, executive functioning, and visual reaction time (30). In a familial study of three persons who were found to be acallosal, difficulties with memory and verbal ability were shown (31). The steepest declines, along with the greatest deviations from normal development, among the medulloblastoma patient group of the present study occurred in the most posterior subregion of the corpus callosum: the splenium. A recent study of patients with callosal lesions showed a clear relation between splenium lesions and left ear suppression of consonant-vowel syllables in a dichotic listening task (32). The authors speculate that damage to the splenial region of the corpus callosum resulted in disruption to the interhemispheric transfer of auditory information.

The present results serve as a foundation for future studies of lesion-behavior relationships with irradiation dose maps to evaluate dose-tissue response. Confirmation of early signs of tissue injury during CSI that increase the risk for later neurocognitive problems may stimulate reconsideration of the treatment plan and initiation of appropriate cognitive remediation programs. Future studies using dosimetry mapping of irradiation disbursement along with specific neurocognitive evaluation among this population are planned.

Conclusion

In the normal brain, corpus callosum continues to develop in an anterior to posterior pattern well into the 2nd decade of life. In the present study, however, patients with medulloblastoma showed a decline in corpus callosum volume during a 4-year period starting with initiation of CSI therapy. Although the most anterior regions of the corpus callosum did not significantly deviate from normal development, the most posterior regions of the corpus callosum showed the greatest declines and the greatest deviations from normal development. Because the tumor bed is in the posterior fossa region, the posterior regions of the corpus callosum receive a higher concentration of irradiation. The subregion-specific changes in corpus callosum volume suggest a differential response to CSI dose exposure. Damage to the corpus callosum interferes with the function of interhemispheric pathways. Performance of patients with medulloblastoma on neurocognitive tasks requiring interhemispheric transfer of information warrants future investigation. Confirmation of such relationships could stimulate development of alternative treatment plans and application of cognitive rehabilitation programs specifically tailored for these patients.

References

1. Constine LS, Konski A, Ekholm S, McDonald S, Rubin P. **Adverse effects of brain irradiation correlated with MR and CT imaging.** *Int J Radiat Oncol Biol Phys* 1988;15:319–330.
2. Mulhern RK, Reddick WE, Palmer SL. **Neurocognitive deficits in medulloblastoma survivors are associated with white matter loss.** *Ann Neurol* 1999;46:834–841.
3. Reddickaij WE, Russell JM, Glass JO, et al. **Subtle white matter volume differences in children treated for medulloblastoma with conventional or reduced dose craniospinal irradiation.** *Magn Reson Imaging* 2000;18:787–793.
4. Schultheiss TE, Kun LE, Ang KK, Stephens LC. **Radiation response of the central nervous system.** *Int J Radiat Oncol Biol Phys* 1995;31:1093–1112.
5. Giedd JN, Blumenthal J, Jeffries NO, et al. **Development of the human corpus callosum during childhood and adolescence: a longitudinal MRI study.** *Prog Neuropsychopharmacol Biol Psychiatry* 1999;23:571–588.
6. Reddick WE, Glass JO, Cook EN, Elkin TD, Deaton RJ. **Automated segmentation and classification of multispectral magnetic resonance images of brain using artificial neural networks.** *IEEE Trans Med Imaging* 1997;16:911–918.
7. Reddick WE, Mulhern RK, Elkin TD. **A hybrid neural network analysis of subtle brain volume differences in children surviving brain tumors.** *Magn Reson Imaging* 1998;16:413–421.
8. Giedd JN, Rumsey JM, Castellanos FX, et al. **A quantitative MRI study of the corpus callosum in children and adolescents.** *Brain Res Dev Brain Res* 1996;91:274–280.
9. Mulhern RK, Palmer SL, Reddick WE, et al. **Risks of young age for selected neurocognitive deficits in medulloblastoma are associated with white matter loss.** *J Clin Oncol* 2001;19:472–479.
10. Palmer SL, Goloubeva O, Reddick WE, et al. **Patterns of intellectual development among survivors of pediatric medulloblastoma: a longitudinal analysis.** *J Clin Oncol* 2001;19:2302–2308.
11. Gajjar A. **Recent advances in therapy for medulloblastoma.** In: *American Society of Clinical Oncology 1999 Spring Educational Book.* Alexandria: *American Society of Clinical Oncology* 1999:579–586.
12. Strother D, Ashley D, Kellie SJ, et al. **Feasibility of four consecutive high-dose chemotherapy cycles with stem-cell rescue for patients with newly diagnosed medulloblastoma or supratentorial primitive neuroectodermal tumor after craniospinal radiotherapy: results of a collaborative study.** *J Clin Oncol* 2001;19:2696–2704.
13. Witelson SF. **Hand and sex differences in the isthmus and genu of**

the human corpus callosum: a postmortem morphological study. *Brain* 1989;112:799–835.
14. Rosenthal R, Rosnow RL. ***Essentials of Behavioral Research: Methods and Data Analysis.*** New York: McGraw-Hill, Inc.; 1991.
15. Chambers JM, Hastie TJ. ***Statistical Models in Southern California.*** Pacific Grove: Wadsworth & Brooks; 1993.
16. Jones RH. ***Longitudinal Data with Serial Correlation: A State-Space Approach.*** London: Chapman and Hall; 1993.
17. Little RC, Milliken GA, Stroup WW. ***SAS System for Mixed Models.*** Carey: SAS Institute; 1996.
18. Rutter CM, Elashoff RM. **Analysis of longitudinal data: random coefficient regression modeling.** *Stat Med* 1994;13:1211–1231.
19. Searle SR. ***Linear Models for Unbalanced Data.*** New York: Wiley; 1987.
20. Venables WN, Ripley BD. ***Modern Applied Statistics.*** New York: Springer-Verlag; 1997.
21. Juraska JM, Kopcik JR. **Sex and environmental influences on the size and ultrastructure of the rat corpus callosum.** *Brain Res* 1988;450:1–8.
22. Abreu-Villaca YY, Schmidt SL. **Effects of prenatal gamma irradiation on the development of the corpus callosum of Swiss mice (abstr).** *Int J Dev Neurosci* 1999;17:693–704.
23. Barkovich AJ. **Concepts of myelin and myelination in neuroradiology.** *AJNR Am J Neuroradiol* 2000;21:1099–1109.
24. Eliez S, Reiss AL. **Annotation: MRI neuroimaging of childhood psychiatric disorders: a selective review.** *J Child Psychol Psychiatry* 2000;41:679–694.
25. Hardan AY, Minshew NJ, Keshavan MS. **Corpus callosum size in autism.** *Neurology* 2000;55:1033–1036.
26. Giedd JN, Castellanos FX, Casey BJ, et al. **Quantitative morphology of the corpus callosum in attention deficit hyperactivity disorder.** *Am J Psychiatry* 1994;151:665–669.
27. Baumgardner TL, Singer HS, Denckla MB, et al. **Corpus callosum morphology in children with tourette syndrome and attention deficit hyperactivity disorder.** *Neurology* 1996;47:477–482.
28. Hynd GW, Semrud-Clikeman M, Lorys AR. **Corpus callosum morphology in attention deficit-hyperactivity disorder: morphometric analysis of MRI.** *J Learn Disabil* 1991;24:141–146.
29. Schmitt JE, Eliez S, Warsofsky IS, Bellugi U, Reiss AL. **Corpus callosum morphology of Williams syndrome: relation to genetics and behavior.** *Dev Med Child Neurol* 2001;43:155–159.
30. Verger K, Junque C, Levin HS, et al. **Correlation of atrophy measures on MRI with neuropsychological sequelae in children and adolescents with traumatic brain injury.** *Brain Inj* 2001;15:211–221.
31. Finlay DC, Peto T, Payling J, Hunter M, Fulham WR, Wilkinson I. **A study of three cases of familial related agenesis of the corpus callosum.** *J Clin Exp Neuropsychol* 2000;22:731–742.
32. Pollman S, Maertens M, von Cramon DY, Lepsien J, Hugdahl K. **Dichotic listening in patients with splenial and nonsplenial callosal lesions.** *Neuropsychology* 2002;16:56–64.